Photomosaics of the cathodoluminescence of 60 sections of meteorites and lunar samples

D. G. Akridge,[1] J. M. C. Akridge,[2] J. D. Batchelor,[3] P. H. Benoit,[2,4] J. Brewer,[5] J. M. DeHart,[4] B. D. Keck,[6] Lu Jie,[7] A. Meier,[4,5] M. Penrose,[4] D. M. Schneider,[8] D. W. G. Sears,[2,4] S. J. K. Symes,[9] and Zhang Yanhong[10]

Received 9 October 2003; revised 5 February 2004; accepted 14 May 2004; published 30 July 2004.

[1] Cathodoluminescence (CL) petrography provides a means of observing petrographic and compositional properties of geological samples not readily observable by other techniques. We report the low-magnification CL images of 60 sections of extraterrestrial materials. The images we report include ordinary chondrites (including type 3 ordinary chondrites and gas-rich regolith breccias), enstatite chondrites, CO chondrites and a CM chondrite, eucrites and a howardite, lunar highland regolith breccias, and lunar soils. The CL images show how primitive materials respond to parent body metamorphism, how the metamorphic history of EL chondrites differs from that of EH chondrites, how dark matrix and light clasts of regolith breccias relate to each other, how metamorphism affects eucrites, the texture of lunar regolith breccias and the distribution of crystallized lunar spherules ("lunar chondrules"), and how regolith working affects the mineral properties of lunar soils. More particularly, we argue that such images are a rich source of new information on the nature and history of these materials and that our efforts to date are a small fraction of what can be done. *INDEX TERMS:* 3662 Mineralogy and Petrology: Meteorites; 3625 Mineralogy and Petrology: Descriptive mineralogy; 3672 Mineralogy and Petrology: Planetary mineralogy and petrology (5410); 5112 Physical Properties of Rocks: Microstructure; 6094 Planetology: Comets and Small Bodies: Instruments and techniques; *KEYWORDS:* cathodoluminescence, lunar samples, meteorites

Citation: Akridge, D. G., et al. (2004), Photomosaics of the cathodoluminescence of 60 sections of meteorites and lunar samples, *J. Geophys. Res.*, *109*, E07S03, doi:10.1029/2003JE002198.

1. Introduction

[2] Cathodoluminescence (CL) is the production of light by a sample in response to exposure to a beam of electrons [*Marshall*, 1988; *Pagel et al.*, 2000]. The phenomenon was described by William Crookes soon after the discovery of the electron and cathodoluminescent materials were essential for the invention of the Crookes tube (the cathode ray tube). However, Edward Charles Howard (after whom we have the "howardites") might have been the first to observe the cathodoluminescence of meteorites in his chemical investigations of "atmospheric stones" almost a century earlier [*Howard*, 1802]. Howard wrote:

> I ought not to suppress, that in endeavouring to form an artificial black coating on the interior surface of one of the stones from Benares, by sending over it the electrical charge of about 37 square feet of glass it was observed to become luminous, in the dark, for nearly a quarter on an hour: and that the tract of the electrical fluid was rendered black.

The wavelength of the light emitted depends mainly on the composition and crystallographic structure of the material producing the light [*Burns*, 1969], although there is some evidence the energy of the electron beam can also influence wavelength of the CL. Cathodoluminescence was first applied to geological studies in a systematic way in the mid-1960s [e.g., *Smith and Strenstrom*, 1965; *Sippel and Spencer*, 1970] and has since been used extensively as a tool for sedimentary petrography [e.g., *Marshall*, 1988; *Stevens Kalceff et al.*, 2000; *Machel*, 2000]. Imaging of zircons with CL prior to U-Pb dating with ion microprobe techniques is now a standard procedure. Considerable progress has been made in recent years in understanding luminescence mechanisms for geological materials [*Burns*, 1969; *Pagel et al.*, 2000]. A recent example is the identification of shocked quartz from potential terrestrial impact craters [*Boggs et al.*, 2001].

[1]Process Dynamics, Fayetteville, Arkansas, USA.
[2]Arkansas-Oklahoma Center for Space and Planetary Sciences, University of Arkansas, Fayetteville, Arkansas, USA.
[3]Department of Science, Community College of Southern Nevada, Cheyenne Campus, Las Vegas, Nevada, USA.
[4]Department of Chemistry and Biochemistry, University of Arkansas, Fayetteville, Arkansas, USA.
[5]Department of Mathematics, Emory College, Atlanta, Georgia, USA.
[6]Procter and Gamble, Cincinnati, Ohio, USA.
[7]World Minerals Inc., Lompoc, California, USA.
[8]Chemistry Department, Southwest Missouri State University, Springfield, Missouri, USA.
[9]Department of Chemistry, University of Tennessee, Chattanooga, Tennessee, USA.
[10]Indiana Geological Survey, Indiana University, Urbana-Champaign, Indiana, USA.

0148-0227/04/2003JE002198$09.00

Table 1. Samples, Source, Microprobe Section Catalog Number, and Cathodoluminescence Figure Number in the Accompanying Auxiliary Material[a]

Sample	Source/Catalog Number	Figure Number
Carbonaceous Chondrites		
Murchison (CM2)	AMNH 4377-2	A1
Colony (CO3.0)	UNM 826	A2
Allan Hills A77307 (CO3.1)	JSC	A3
Kainsaz (CO3.2)	AMNH 4717-1	A4
Lancé (CO3.4)	UNM 824	A5
Allan Hills A77003 (CO3.4)	JSC	A6
Isna (CO3.7)	UNM 825	A7
Ordinary Chondrites		
Semarkona (LL3.0)	Uark	A8
Semarkona (LL3.0)	NMNH 4128-1	A9
Semarkona (LL3.0)	UNM 549	A10
Semarkona (LL3.0)	UNM 549	A11
Semarkona (LL3.0)	UNM 620A	A12
Semarkona (LL3.0)	UNM 620B	A13
Krymka (LL3.1)	NMNH 1729-8	A14
Bishunpur (LL3.1)	NHM, P18	A15
Roosevelt County 075 (H3.1)	UH 82	A16
St. Mary's County (LL3.3)	NMNH 5423-1	A17
Allan Hills A77214 (LL3.4)	JSC (8)	A18
Chainpur (LL3.4)	NHM P42	A19
Yamato 790448 (LL3.6)	NIPR	A20
Hedjaz (L3.7)	NHM, P30	A21
Ngawi (LL3.2/3.7)	NHM, P103	A22
Mezö-Madaras (LL3.4/3.7)	NHM, P60	A23
Dhajala (H3.8)	PRL	A24
Acfer 028 (H4)	UM, PL 91093	A25
Allan Hills 81029 (H4)	JSC (1,11)	A26
Fayetteville (regolith breccia) Uark	(JSC38,212 or JSC23,54)	A27
Plainview (regolith breccia)	NMNH 3417	A28
Enstatite Chondrites		
Allan Hills 84206 (EH3)	JSC	A29
Allan Hills 84170 (EH3)	JSC	A30
Pecora Escarpment 91085 (EH4)	JSC	A31
Pecora Escarpment 91238 (EH4)	JSC	A32
Saint-Sauveur (EH5) MNHN	L 1456A	A33
Lewis Cliff 88180 (EH5)	JSC (1,13)	A34
Allan Hills 85119 (EL3)	JSC (1,11)	A35
MacAlpine Hills 88184 (EL3)	JSC (1,21)	A36
MacAlpine Hills 88136 (EL3)	JSC (20,34)	A37
Thiel Mountains 91714 (EL5)	JSC	A38
Reckling Peak A80259 (EL5)	JSC (5,26)	A39
Allan Hills 81021 (EL6)	JSC (19,44)	A40
Atlanta (EL6)	UL	A41
Khairpur (EL6)	UL	A42
Lewis Cliff 88135 (EL6)	JSC	A43
Lewis Cliff87119 (EL6)	JSC	A44
Lewis Cliff 87223 (EL3 anom)	JSC	A45
Happy Canyon (EL anom)	UL	A46
Eucrites and Howardite		
Pasamonte (eucrite type 2)	NMNH 897-2	A47
Pasamonte (eucrite type 2)	NMNH 897-2	A48
Juvinus (eucrite type 5)	AMNH 439-1	A49
Kapoeta (howardite)	AMNH 4846	A50
Lunar Highland Regolith Breccias		
14318 Apollo lunar sample (highland regolith breccia)	JSC (48)	A51
14318 Apollo lunar sample (highland regolith breccia)	JSC (48)	A52
14135 Apollo lunar sample (highland regolith breccia)	JSC (20)	A53
14318 Apollo lunar sample (highland regolith breccia)	JSC (6)	A54
Pristine Highland Sample		
60015 Apollo lunar sample (pristine highland sample)	JSC (757)	A55
Lunar Soils		
60009 Apollo lunar sample (Apollo 16 drive tube)	JSC (6028)	A56
60009 Apollo lunar sample (Apollo 16 drive tube)	JSC (6028)	A57
60009 Apollo lunar sample (Apollo 16 drive tube)	JSC (6019)	A58
60009 Apollo lunar sample (Apollo 16 drive tube)	JSC (6019)	A59
60010 Apollo lunar sample (Apollo 16 drive tube)	JSC (6019)	A60

[a]Abbreviations for sample sources are as follows: AMNH, American Museum of Natural History, New York; JSC, Johnson Space Center, Houston; MNHN, Museum National d'Histoire Naturelie, Paris; NHM, Natural History Museum, London; NIPR, National Institute of Polar Research; PRL, Physical Research Lab, Ahmedabad, India; Uark, University of Arkansas, Fayetteville; UH, University of Hawaii, Manoa; UL, University of Leicester; UM, University of Münster; UNM, University of New Mexico; Albuquerque.

[3] The luminescence mechanism usually involves the excitation of electrons in a mineral structure, and subsequent emission of photons as the excited electrons return to the ground state. While this process is well understood for free atoms, and forms the basis of a variety of analytical techniques for measuring chemical composition, the situation is more complicated for atoms in a solid state crystal [*Burns*, 1969]. In such cases, luminescence may involve either intrinsic properties of the lattice, such as lattice defects, or it can involve impurities in the crystal structure that can act either as "activators" [e.g., *Krbetscheck et al.*, 1997; *Götze et al.*, 2000] or "quenchers" [e.g., *Telfer and Walker*, 1978; *Götze et al.*, 2000]. Research on synthetic materials shows that trace amounts of some activator ions can be sufficient to produce radical changes in luminescence properties and some ions can act as either quenchers or activators depending on their placement in the crystal lattice or their abundance. The presence of unanticipated activators or quenchers complicates the determination of mineralogy and mineral chemistry from luminescence properties.

[4] Most studies of the CL of extraterrestrial materials have concentrated on individual phases or grains. We have concentrated on the CL properties of entire sections so that we could investigate the macroscopic petrography of the sections and the history the section as a whole. We here report data for 60 of the over 185 sections we have recorded in the last 20 years. By taking a large number of photographic images, we have been able to assemble mosaics of an entire thin section of moderately high resolution. In this way the texture, mineralogy and mineral composition of an entire section can be examined in a fashion not possible by other techniques. Thus, for example, the distribution and type of components in a section is easily visible because in

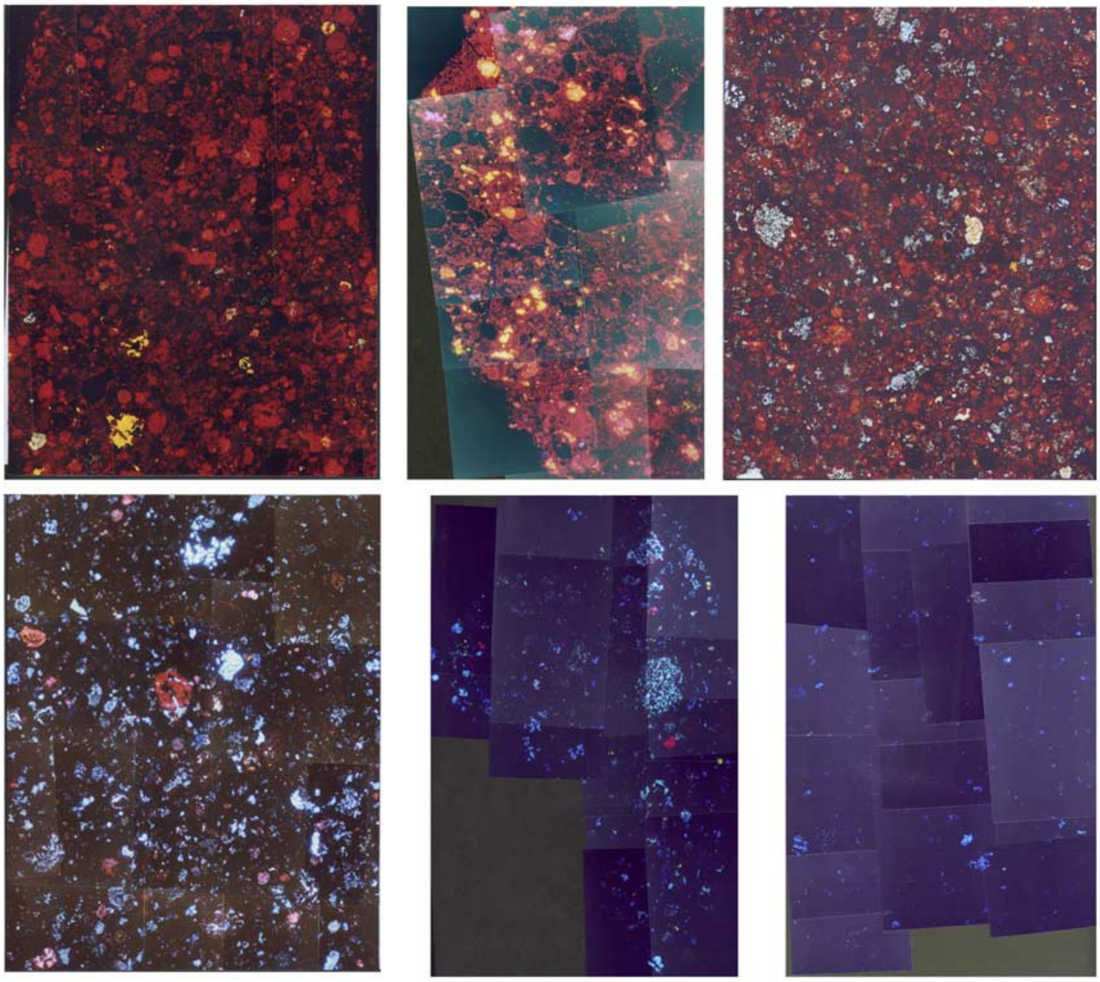

Figure 1. Cathodoluminescence mosaics of six CO chondrites. From top left to bottom right the meteorites are Colony (type 3.0), Allan Hills A77307 (type 3.1), Kainsaz (type 3.2), Lancé (type 3.4), Allan Hills A77003 (type 3.4), and Isna (type 3.7). The images are typically about a centimeter across.

addition to textural differences these components will differ (sometimes markedly) in CL properties. We have found the photomosaics especially informative when combined with our efforts to understand the thermoluminescence (TL) properties, and thus the thermal and metamorphic history of these materials. We suggest that with a little coaching in the CL properties of minerals, researchers with interests different from ours will be able to use these photomosaics to find new insights into the history of these materials.

2. Instrumentation, Procedures, and Samples

[5] Our CL images were produced using a MAAS Luminoscope© attached to a standard petrographic microscope. The electron gun was typically operated at 15 ± 1 keV and 0.7 ± 0.1 mA and the beam focused to a 1×2 cm ellipse. The images were recorded using standard color film, typically 400 speed, processed commercially using the C-40 process. A typical thin section required about 40 images. Photomosaics were assembled from the prints and scanned with large flatbed scanner. The exposure time for each image was adjusted to suit the luminescence intensity of the sample and varied from 15 seconds to 7 minutes. Thus intensity of the photographic images does not reflect CL intensity. A list of samples whose CL is reported here is given in Table 1, along with details of class and petrographic type, source, and section number. The CL images appear in the accompanying auxiliary material[1], and a sampling of six mosaics appears in Figure 1. These mosaics are typically 10 mm in their shortest dimension.

[6] After perusing the images for details, it was thought helpful to summarize color trends in a quantitative way by defining "color indices." Using the Adobe Photoshop 5.0 image analysis program the whole image was selected and the mean color values and standard deviation recorded for the red, blue and green pixels. The color indices are the ratio of color values obtained this way (Table 2).

3. Cathodoluminescence Properties of Major Meteorite Groups

[7] We will review the CL properties of each of our 60 sections. In our descriptions we will sometimes refer to

[1]Auxiliary material is available at ftp://ftp.agu.org/apend/je/2003JE002198.

Table 2. Color Index Data for CL Mosaics

	Brightness Value							
	Luminosity		Red		Green		Blue	
Sample	Mean	σ	Mean	σ	Mean	σ	Mean	σ
Carbonaceous Chondrites								
1 Murchison	64	25	127	63	32	15	64	10
2 Colony	55	30	111	62	29	27	45	19
3 ALHA77307	66	34	132	66	35	33	49	20
4 Kainzaz	57	38	101	53	35	42	55	35
5 Lance	56	44	73	35	49	49	55	62
6 ALHA77003	69	38	53	25	74	47	85	48
7 Isna	77	19	84	15	66	22	115	19
Ordinary Chondrites								
8 Semarkona (1)	59	39	62	62	58	33	55	32
9 Semarkona (2)	29	27	62	57	15	25	15	17
10 Semarkona (3)	52	44	95	58	31	47	41	40
11 Semarkona (4)	37	24	62	52	25	22	34	12
12 Semarkona (5)	47	30	80	59	31	28	45	13
13 Semarkona (6)	43	29	55	68	38	20	39	12
14 Krymka	57	44	76	50	45	44	61	48
15 Bishunpur	43	37	46	48	42	34	38	37
16 Roosevelt County	73	41	100	49	60	44	70	47
17 St Mary's County	58	37	54	31	56	43	81	46
18 ALHA 77214	69	36	81	29	62	40	66	52
19 Chainpur	60	48	59	44	56	49	79	64
20 Yamato 790448	51	44	65	40	43	50	58	53
21 Hedjaz	84	33	96	22	78	36	82	59
22 Ngawi	80	48	88	44	74	52	89	50
23 Mezo Madaras	66	44	69	36	63	49	74	56
24 Dhajala	70	38	80	25	56	45	120	48
25 Acfer 028	112	52	126	38	103	58	119	60
26 ALH 81029	112	57	112	41	65	94	126	66
27 Fayetteville	79	44	44	28	89	56	120	66
28 Plainview	85	46	62	24	91	59	123	66
Enstatite Chondrites								
29 ALH 84206	64	26	104	64	45	16	53	18
30 ALH 84170	120	28	141	67	114	18	92	20
31 PCA 91085	108	25	144	62	93	16	87	25
32 PCA 91238	113	38	135	73	107	26	92	31
33 St. Sauveur	68	30	33	23	66	39	177	50
34 LEW 88180	100	29	72	51	108	26	133	46
35 ALH 85119	99	34	133	69	86	25	79	29
36 MAC 88184	112	34	198	48	69	29	111	52
37 MAC 88136	86	20	193	27	32	20	81	38
38 TIL 91714	125	31	167	60	106	21	108	26
39 RKPA80259	93	22	213	42	34	15	83	41
40 ALH 81021	116	32	166	59	91	23	113	28
41 Atlanta	118	30	155	54	98	21	98	21
42 Khairpur	106	153	64	20	85	20	91	31
43 LEW 88135	118	40	194	49	81	39	109	50
44 LEW 87119	123	29	155	59	109	18	110	18
45 LEW 87223	93	24	201	47	40	18	83	33
46 Happy Canyon	87	34	132	77	67	17	70	29
HED Meteorites								
49 Juvinas	105	54	137	65	98	58	60	10
47 Pasamonte (1)	99	49	136	31	82	52	88	12
48 Pasamonte (2)	88	44	121	57	73	46	76	11
50 Kapoeta	88	52	105	55	79	58	88	15
Lunar Samples								
51 14318, 48 (1)	121	50	125	40	118	55	127	57
52 14318, 48 (2)	123	47	130	37	120	53	126	55
53 14135, 20	120	43	132	39	116	46	105	47
54 14318, 6	117	49	126	39	114	54	112	59
55 60015, 757	167	27	176	23	172	28	119	39
56 60009, 6028 (1)	140	50	159	49	134	54	119	42
57 60009, 6028 (2)	130	56	137	56	128	60	105	47
58 60009, 6019 (1)	117	58	135	54	111	63	107	51
59 60009, 6019 (2)	122	65	135	68	116	71	118	68
60 60010, 6019	103	61	118	57	96	64	96	52

mineralogy and mineral chemistry. Unless otherwise stated, these mineral identifications are based on luminescence properties rather than optical petrography or electron microprobe analysis. We feel that this subject has advanced far enough to permit this approach, but it should be stressed that many of these sections have been the subject of deeper study and details are given in the references quoted. For overviews of meteorite mineral CL, the reader is referred to *Marshall* [1988] and *Steele* [1990]. Throughout our descriptions we will refer to the chondrule classes defined by *Sears et al.* [1992]. This scheme is based entirely on mineral and phase chemistry and is especially well-suited to CL studies. It will be described in greater detail below.

3.1. Carbonaceous Chondrites (Cathodoluminescence Images 1–7)

[8] Two classes of carbonaceous chondrites are represented in our study, the CM chondrites by a lone image of Murchison (Figure A1) and the CO chondrites by Colony (CO3.0, Figure A2), Allan Hills A77307 (CO3.1, Figure A3), Kainsaz (CO3.2, Figure A4), Lancé (CO3.4, Figure A5), Allan Hills A77003 (CO3.4, Figure A6), Isna (CO3.7, Figure A7). The CL properties of Murchison were discussed by *Sears et al.* [1993] and the CL properties of CO chondrites were discussed by *Sears et al.* [1991]. The CL mosaics for the six CO chondrites are also shown in Figure 1.

[9] The sea of red grains in the Murchison mosaic (Figure A1) is largely due to the iron-free olivine. Some of the large dark areas are olivines that contain Fe, the Fe quenching the luminescence [*Steele*, 1986, 1989]. Thus the chondrules that contain olivine with more than a percent or so of Fe are readily distinguishable from the usually larger chondrules that are Fe-poor. The olivines in CM chondrites were divided into Fe-rich and Fe-poor varieties by *Wood* [1962] and *McSween et al.* [1977a, 1977b]. The larger Fe-poor chondrules are usually surrounded by thick fine-gained rims of material that contain microscopic red grains of olivine [*Tomeoka and Buseck*, 1985; *Metzler et al.*, 1992; *Sears et al.*, 1993]. The chondrules that appear dark due to their Fe-bearing olivines also have fine-grained rims, but their rims are much thinner. There are about 12 examples in Figure A1. Murchison, like most of the CM chondrites, has been penetrated by water and this has reacted with some of the chondrules to give them an eroded appearance (an example appears at the top center of Figure A1). The occasional yellow grain is mostly glass, but some zoned refractory inclusions of calcium-rich minerals also have yellow CL. An example of a highly luminescent zoned yellow-red refractory grain appears in the lower central part of Figure A1.

[10] The appearance of the CO chondrites in the CL microscope depends on their petrographic type (Figure 1) [*Sears et al.*, 1991]. Colony and Allan Hills are of low type and, like Murchison, contain abundant red CL due to iron-free olivine (Figures A2 and A3). However, iron has diffused into about half of the grains, making their CL less intense. The two fragments of yellow glass appear to be chondrule fragments. Kainsaz has abundant red grains with a range of intensities. These are olivine grains that are losing their luminescence as iron diffuses into them. There are also a few grains with blue CL. These are feldspar grains

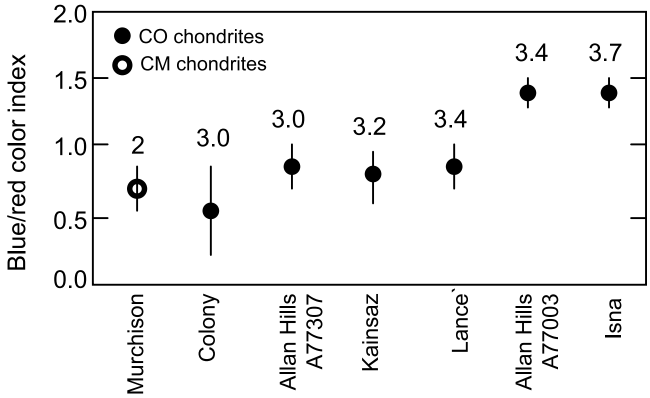

Figure 2. Blue to red color index (ratio of the number of blue pixels to the number of red pixels in the digital image) for the CL images of C chondrites. The color index increases as a function of petrologic type. Detailed studies suggest that this trend reflects the destruction of forsterite with red CL and creation of crystallized feldspar with blue CL in response to metamorphism.

that appear as glass crystallizes during metamorphism (Figure A4). As petrographic type increases (see Lancé, type 3.4, ALHA77003, type 3.4, and Isna, type 3.7, Figures A5–A7), the blue CL of the feldspar continues to increase while the olivine loses its red CL. It is thus possible to define a color index on the basis of the relative proportions of blue and red CL in the section. This color index increases with petrographic type (Figure 2).

[11] The CL of two CV chondrites (Axtell and Coolidge) was described by *Guimon et al.* [1995]. These meteorites exhibited very little CL and had non-luminescent matrices. The brightest CL associated with these meteorites was from CAI, although many CAI were nonluminescent. A few chondrules in Axtell resembled (in CL properties) group A3 chondrules in ordinary chondrites, but most were most like the nonluminescent group B1 and B2 chondrules. In contrast, chondrules in Coolidge most closely resemble A5 or B3 chondrules in ordinary chondrites.

3.2. Ordinary Chondrites (Cathodoluminescence Figures A8–A28)

[12] We present six images of Semarkona (LL3.0) (Figures A8-13). The other ordinary chondrites are Krymka (LL3.1, Figure A14), Bishunpur (LL3.1, Figure A15), Roosevelt County 075 (H3.1, Figure A16), St Mary's County (LL3.3, Figure A17), Allan Hills A77214 (LL3.4, Figure A18), Chainpur (LL3.4, Figure A19), Yamato 790448 (LL3.0, Figure A20), Hedjaz (L3.7, Figure A21), Ngawi (an LL chondrite breccia of mean petrographic type 3.7 but containing clasts of type 3.2, Figure A22), Mezö-Madaras (a breccia of LL3.4 and LL3.7, Figure A23), Dhajala (H3.8, Figure A24), Acfer 028 (H4, Figure A25) and Allan Hills 81029 (H4, Figure A26). In addition, we include images of two gas-rich regolith breccias, Fayetteville (Figure A27) and Plainview (Figure A28).

[13] Semarkona is unique in its CL properties as it is in many chemical, isotopic and mineralogical properties [e.g., *Sears et al.*, 1990; *Matsunami et al.*, 1993]. Large chondrules and other structural components in Semarkona are surrounded by a fine-gained (almost "smoky") matrix with red CL characteristic of Fe-free olivine. In this respect, the CL images of Semarkona (Figures A8–A13) resemble those of Murchison (Figure A1), Colony (Figure A2) and Allan Hills A77307 (Figure A3), that are classes CM2, CO3.0 and CO3.1, respectively. The nearest ordinary chondrite relatives to Semarkona, Krymka (Figure A14), Bishunpur (Figure A15) and Roosevelt County 075 (Figure A16), that are classes LL3.1, LL3.1 and H3.1, respectively, have matrix with very different CL properties. In most ordinary chondrites the fine-gained matrix is essentially dark. As with the CO chondrites, the cathodoluminescence changes steadily with petrographic type, yellows and reds of calcium-rich glasses and olivines disappearing and the amount of blue due to feldspar increasing. St. Mary's County (Figure A17), Allan Hills A77241 (Figure A18) and Chainpur (Figure A19), that are classes LL3.2, LL3.4 and LL3.4, respectively, contain chondrules with blue cathodoluminescence and non-luminescent matrix. The remaining meteorites (Yamato 790448, Hedjaz, Ngawi, Mezö-Madaras, Dhajala, Acfer 028 and Allan Hills 81029, Figures A20–A26) continue the trend of greater amounts and brighter levels of blue luminescence from the feldspars. *Scott et al.* [1988] reviewed the mineralogy and petrology of the fine-grained matrix in primitive meteorites.

[14] Again as with CO chondrites, it is possible to define a color index for ordinary chondrites that increases with petrographic type (Figure 3).

[15] Cathodoluminescence is particularly well-suited to observing the textural and compositional diversity of chondrules and tracking changes during metamorphism (Figure 4) [*Sears et al.*, 1995]. *Sears et al.* [1992] and *DeHart et al.* [1992] identified 8 classes of chondrules in type 3 ordinary chondrites on the basis of their CL properties and then defined these in terms of the composition of the olivine grains and mesostasis (Table 3). *Huang et al.* [1996] compared the scheme with other chondrule classification schemes. These chondrule classes can be seen in Figures A8–A28. Four of the chondrule classes are primary

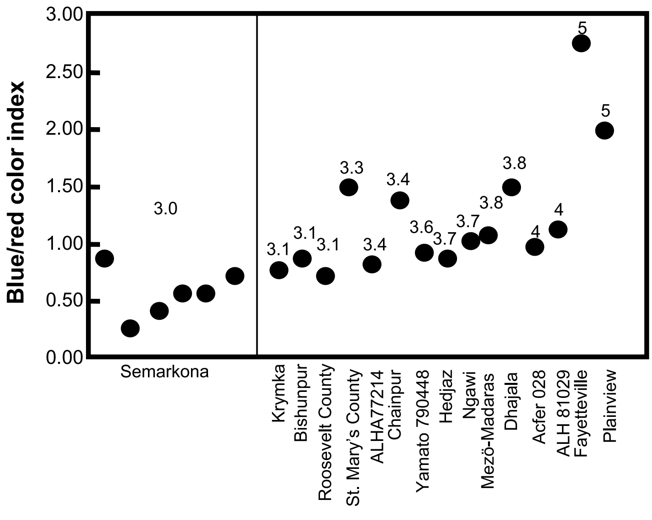

Figure 3. Blue to red color index for ordinary chondrites. As with C chondrites (Figure 1), the color index increases as a function of petrologic type as forsterite is destroyed and feldspar crystallizes in response to metamorphism.

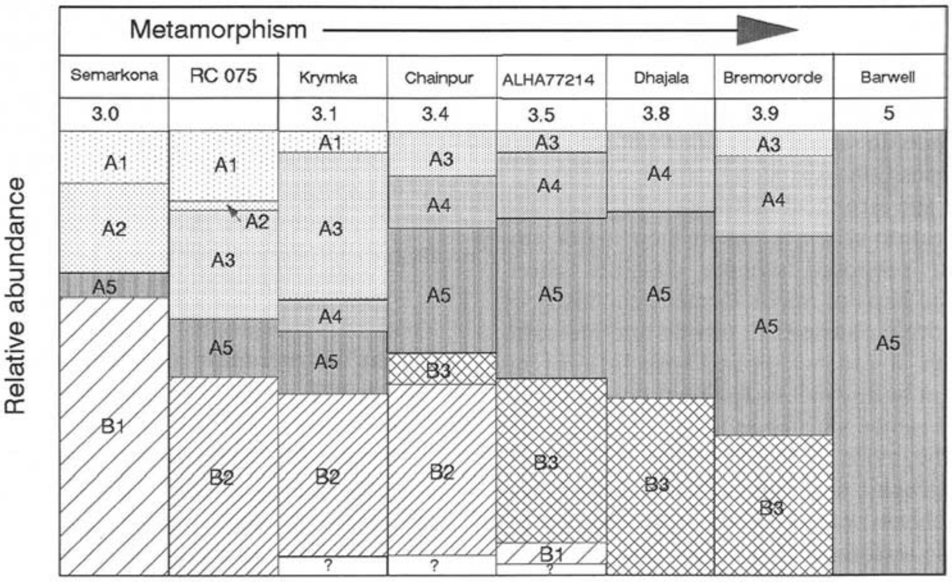

Figure 4. Abundance of chondrule types as a function of petrographic type from *Sears et al.* [1995]. It can be deduced from these data that Roosevelt County is type 3.1 [see also *McCoy et al.*, 1993]. Chondrules in unmetamorphosed meteorites are highly diverse in their mineralogical properties, and this is reflected in their CL properties. On the other hand, chondrules in metamorphosed meteorites are uniform in their mineralogical and CL properties. See Table 2 for an explanation of the chondrule classes. Significantly, some of these "equilibrated" (A5) chondrules are found in even the least metamorphosed meteorites although they show considerable compositional heterogeneity.

(i.e., existed prior to the final aggregation of the meteorite and thus abundant in the low petrographic types) and four are formed as a result of metamorphic alteration and are seen at various petrographic levels throughout the sequence. The final fate of all chondrules is to be compositionally uniform and of a single class (so-called class A5).

[16] Brecciation is common among meteorites of all classes, and when components of low but different petrographic type are mixed it is easy to see in these CL images. Ngawi is a mixture of type 3.2 material (most of Figure A22) with low levels of CL surrounded by a mixture that on average has very relatively high levels of CL (bottom left corner of Figure A22). This mixture contains chondrules typical of low petrographic types like Semarkona. Mezö-Madaras is also a breccia of material with different petrographic types, but none of the material is low enough in petrographic type to produce the marked difference in CL properties observed in Ngawi.

[17] Finally, there are the Fayetteville and Plainview regolith breccias (Figures A27 and A28). These are breccias with clasts of normal material sitting in a matrix of material rich in solar wind noble gases. What is remarkable about these images is that the light clasts and dark matrix look so similar in CL, a clear indication that the matrix is produced by comminuting the clasts, rather than being a new kind of primitive ordinary chondrite material like Semarkona [*Haq et al.*, 1989; *DeHart and Sears*, 1988].

3.3. Enstatite Chondrites (Cathodoluminescence Figures A29–A46)

[18] The accompanying auxiliary material contains CL photomosaics of Allan Hills 84206 (EH3, Figure A29), Allan Hills 84170 (EH3, Figure A30), Pecora Escarpment 91085 (EH4, Figure A31), Pecora Escarpment 91238 (EH4, Figure A32), Saint-Sauveur (EH5, Figure A33), Lewis Cliff 88180 (EH5, Figure A34), Allan Hills 85119 (EL3, Figure A35), MacAlpine Hills 88184 (EL3, Figure A36), MacAlpine Hills 88136 (EL3, Figure A37), Thiel Mountains 91714 (EL5, Figure A38), Reckling Peak 80259 (EL5, Figure A39), Allan Hills 81021 (EL6, Figure A40), Atlanta (EL6, Figure A41), Khairpur (EL6, Figure A42), Lewis Cliff 88135 (EL6, Figure A43), Lewis Cliff 87119 (EL6, Figure A44), Lewis Cliff 87223 (EL3 anomalous, Figure A45), Happy Canyon (EL anomalous, Figure A46). These images are from the work of *Zhang et al.* [1996], who obtained CL images of 10 EH chondrites, 12 EL chondrites, and 5 aubrites, and Happy Canyon.

[19] The cathodoluminescence of the enstatite chondrites is dominated by enstatite that, because it is virtually always

Table 3. Definition of Chondrule Groups in Ordinary Chondrites, Based on Cathodoluminescence Properties[a]

Chondrule Group	CL Color: Olivine	CL Color: Mesostasis
A1	red	yellow
A2	none/dull red	yellow
A3	red	blue
A4	none/dull red	blue
A5	none	blue
B1	none/dull red	none/dull blue
B2	none/dull red	dull blue
B3	none	purple

[a]Approximate phase compositions: normative mesostasis: A1, A2, A3, A4 An > 50%; A5 An < 50%; B1 qtz > 30%; B2 qtz 30–50%; B3 qtz 15–30%. Olivine composition, %FeO: A1 < 2%; A2 2–4%; A3 < 4%; A4, A5 > 4%; B1 4–25%; B2 10–25%; B3 15–20%.

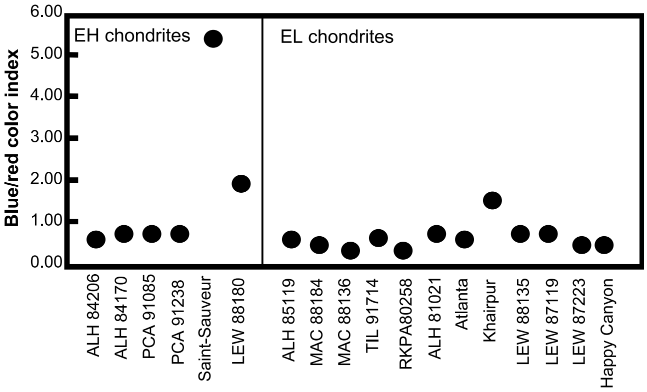

Figure 5. Blue to red color index for enstatite chondrites. For EH chondrites the index increases with petrographic type, but this is not true of EL chondrites. This difference in CL trends between the EH and EL chondrites does not appear to reflect difference in mineral chemistry but seems to be related to difference in thermal history and pyroxene structure. LEW, Lewis Cliff; MAC, MacAlpine Hills; RCP, Reckling Peak; TIL, Thiel Mountains.

iron-free, produces high levels of luminescence. Some grains with small amounts of iron produce a dull red luminescence and very occasionally the iron will be high enough to quench the cathodoluminescence completely [*Lusby et al.*, 1987; *Weisberg et al.*, 1994]. However, most of the non-luminescent (black) grains in the CL images are metal or sulfide grains. Occasionally, a grain will luminesce blue, especially in Pecora Escarpment 91085 (Figure A31), and a few mesostasis regions produce yellow CL. A few isolated grains with yellow CL were tentatively identified as oldhamite (CaS), but these occurred only in a few samples.

[20] In the low petrographic types chondrules and individual grains have sharp and distinct outlines and are easily seen, but as petrologic type increases boundaries become blurred and these components are more difficult to identify. In the high types, chondrules are difficult or impossible to locate, but the high EH types contain enstatite whose CL is blue, with only an occasional magenta grain (Lewis Cliff 88180, Figure A34 and Saint Sauveur, Figure A33), while the high EL types have enstatite with a uniform magenta CL (Thiel Mountains 91714, Figure A38, Reckling Peak 80259, Figure A39 Allan Hills 81021, Figure A40 Atlanta, Figure A41 Khairpur, Figure A42 Lewis Cliff 88135, Figure A43 Lewis Cliff 87119, Figure A44). A color index of the blue to red ratio for the EL chondrites is thus independent of petrographic type, while for the EH chondrite the color index decreases with petrographic type (Figure 5). As discussed in many papers, this trend does not have a compositional explanation and must reflect differences in the thermal history of the EH and EL classes [*Skinner and Luce*, 1971; *Zhang et al.*, 1996].

[21] Happy Canyon (Figure A46) and Lewis Cliff 87223 (Figure A45) are unusual enstatite chondrites, and their cathodoluminescence images are quite different from the others. Happy Canyon has a texture resembling igneous rocks yet a normal EL composition and Lewis Cliff 87223 seems to be an EL chondrite to which considerable metal has been added and sulfides have been removed. They might be rocks from the EL chondrite asteroid that have been completely or partially melted by impact [*Olsen et al.*, 1977; *Bischoff et al.*, 1992; *McCoy et al.*, 1995].

[22] We have not included aubrites in the auxiliary material, but their cathodoluminescence is also dominated by red- to bluish red-luminescing enstatite grains. Since there are many cathodoluminescent phases in aubrites, a detailed study of this class would be of value.

3.4. Eucrites and a Howardite (Cathodoluminescence Figures A47–A50)

[23] There are two CL mosaics of the Pasamonte eucrite (petrographic type 2, Figures A47 and A48), and one each of the Juvinas meteorite (petrographic type 5, Figure A49) and the Kapoeta (howardite, Figure A50). These are all meteorites thought to have originated on the large asteroid Vesta [*Cruikshank et al.*, 1991].

[24] The Pasamonte meteorite shows the yellow CL characteristic of feldspars containing appreciable amounts of calcium, but the intensity is relatively weak and uneven. It is often almost brown in color. The non-luminescent grains are pyroxene. In some parts of the rocks the grains are large and highly developed crystalline shapes, while other parts contain very small grains. The green mineral is a form of silica [*Batchelor*, 1991]. In contrast, the feldspar in Juvinas has relatively bright yellow CL, the metamorphic equilibration having driven trace amounts of quencher iron out of the feldspar crystals. *Batchelor and Sears* [1991b] suggested that these changes in CL color, or, more precisely, the increase in yellow intensity, were caused by iron quencher ions diffusing out of the feldspar during metamorphism [*Takeda et al.*, 1983; *Batchelor and Sears*, 1991b]. The same mechanism would explain the increase in TL sensitivity with petrographic type [*Batchelor and Sears*, 1991a]. In this instance a color index can be defined by the green -to-blue, integrated over the sections, that increases with petrographic type (Figure 6).

[25] Kapoeta is a regolith breccia and its brecciated texture is apparent in its CL mosaic. Angular fragments of rock are set in a “soil” of fragments of different sorts of material, some (like the red olivine grains) are not charac-

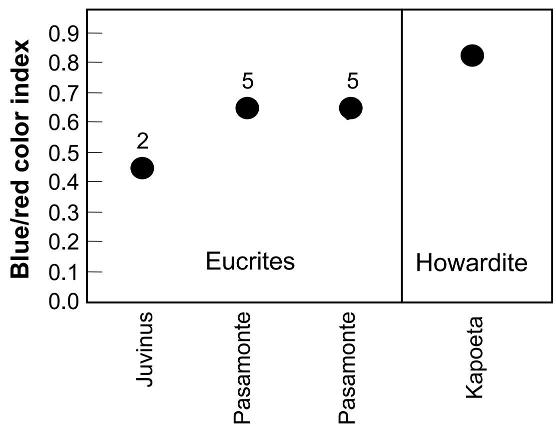

Figure 6. Blue to red color index for two eucrites and a howardite. The feldspar in eucrites decreases in Fe, a quencher of CL, with increasing petrographic type. The feldspar in unmetamorphosed eucrites has a red-brown appearance, whereas the feldspar in metamorphosed eucrites has a bright yellow CL.

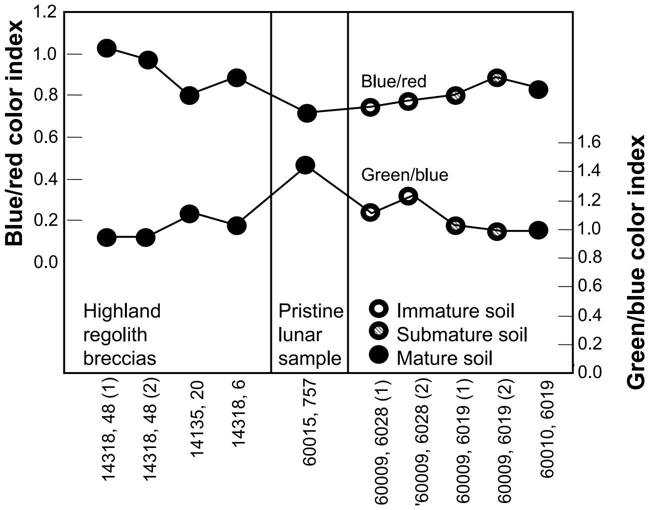

Figure 7. Green to blue and blue/red color index of lunar samples. The two indices are anticorrelated, with green/blue decreasing and blue/red increasing with regolith maturity.

teristic of the rest of the meteorite and probably representing contamination by impact.

3.5. Lunar Highland Breccias (Cathodoluminescence Figures A51–A54)

[26] We include CL photomosaics of three Apollo highland regolith breccias 14318,48 (Figure A51), 14135,20 (Figure A52) and 14318,6 (Figure A54), that were part of a study of the thermal history of the lunar surface by *Batchelor et al.* [1997].

[27] There is a reasonably good understanding of the CL of lunar samples due to the work on the early Apollo samples [*Geake et al.*, 1977; *Sippel and Spencer*, 1970]. Like the eucrites, luminescence in lunar samples is derived largely from feldspar. In samples of highland-dominated Apollo 16 regolith, feldspar grains luminescence yellow-green, or, in some clasts, blue. Feldspar grains exhibiting undulatory extinction or diaplectic glass, reflecting shock processing, are non-luminescent.

[28] The highland regolith breccias are from the Fra Mauro region of the moon. They contain a mixture of rock types, some carried in by the mighty impact that caused the formation of the Imbrium basin. Rock fragments of various sorts can be seen surrounded by a ‘‘matrix’’ of smaller fragments and soil.

[29] Among the matrix components are spherules with yellow CL (or very rarely blue) that contain crystals of calcium-rich feldspar some of which are in the form of needles. These crystallized lunar spherules are very much like the chondrules in meteorites although their compositions are those of the moon rather than being solar or chondritic. It seems that these spherules are melt droplets that were thrown out by the imbrium impact, and probably meteoritic chondrules have a similar origin [*Symes et al.*, 1998; *Ruzicka et al.*, 2000].

[30] We determined both blue/red and green/blue color indices for these and other lunar samples, and these two indices tend to be anticorrelated (Figure 7). The blue/red index decreases and the green/blue index increases along the series 14318,48(1), 14318,48(2), 14135,20 and 14318,6 which reflects the increasing proportion of clast in the section relative to matrix.

3.6. Pristine Highland Sample (Cathodoluminescence Figure A55)

[31] We include a photomosaic of one Apollo pristine highland sample (60015,757, Figure A55).

[32] There is nothing notable about the dull luminescence of this sample, besides its size and uniformity, and it is included for the sake of completeness. The highlands of the moon were so heavily bombarded by meteoroids that it was originally thought impossible to find uncontaminated highland material. However, energetic searching had uncovered a few small samples one of which this is one. These show little evidence for regolith mixing of the sort that produced the regolith breccias above but, are thought to be more like the original igneous rocks that formed the highlands.

[33] The blue/red index reaches minimum and the green/blue index reaches a maximum with this sample (Figure 7).

3.7. Lunar Soils (Cathodoluminescence Figures A56–A60)

[34] Cathodoluminescence images of samples from the Apollo 16 drive core 60009/60010 illustrate the nature of the moon’s soil and how it ‘‘ages’’ (i.e., matures) on the lunar surface. Images 56–60 (Figures A56–A60) are for samples taken from a variety of depths in the regolith. These images and TL sensitivity measurements were discussed by *Batchelor et al.* [1997].

[35] The two mosaics of sample 60009,6028 (Figures A56 and A57) show lunar soil at its most immature, that is, coming from deepest in the core (about 53 cm below the surface) and least affected by the surface processes of bombardment, fragmentation and crushing. Rock fragments, mineral gains and fine soil particles are present in all sizes, and most show fairly high levels of cathodoluminescence. The two mosaics of 60009,6019 (Figures A58 and A59) are from the center of the core (about 29 cm) and are of intermediate maturity. The same mixture of materials is present, but the number of bright yellow gains is fewer giving the whole section is lower level of CL intensity. The single mosaic of 60010,6019 (Figure A60) is from very close to the surface (about 4 cm depth) and shows very little yellow CL. Most of the luminescent gains have been converted to non-luminescent glasses by the impact and surface reworking processes.

[36] The green/blue index decreases and the blue/red index increases with increasing soil maturity. From the CL mosaics it can be seen that this reflects the destruction of crystalline feldspar with yellow-green CL and relative resilience of other cathodoluminescent phases. Thus the overall trend in Figure 7 would seem to reflect mixing between material with CL properties similar to those of the pristine sample and material with relatively low CL and with high blue/red index and low green/blue index. These two components can essentially be identified with clast and matrix.

4. Conclusions

[37] Our goal has been to make available to our colleagues 60 CL mosaics made at great expense (mainly in time) over the last 15 years which we are convinced contain

a wealth of information about the geological history of extraterrestrial samples. We feel we have studied the pictures and written enough research papers on them to demonstrate their utility, but that other researchers with different expertise and interests will find much more of value in the images. We know that there are a number of significant studies to be made, for example, of aqueous alteration effects in Murchison and Semarkona.

[38] We have also identified a series of color indices that can be used to quantitatively assess the level of thermal processes in a variety of extraterrestrial samples. Rock samples that show too little CL for meaningful study are very few, in fact, we are not aware of any (although Martian meteorites come close). Thus by taking a single low resolution image of a centimeter-sized thin section in a CL microscope it will now be possible to quickly and quantitatively determine the thermal alteration of a large number of samples from a given field site.

[39] **Acknowledgment.** We are grateful to Walter Manger of the University of Arkansas' Geology Department for the most generous use of his CL microscope, and we appreciate grant support from the NASA.

References

Batchelor, J. D. (1991), Cathodoluminescence of equilibrated and unequilibrated eucrites and the discovery of multiple silica populations, *Lunar Planet. Sci.*, *XXII*, 61–62.

Batchelor, J. D., and D. W. G. Sears (1991a), Metamorphism of eucrite meteorites studied quantitatively using thermoluminescence, *Nature*, *349*, 516–519.

Batchelor, J. D., and D. W. G. Sears (1991b), Thermoluminescence constraints on the metamorphic, shock, and brecciation history of basaltic meteorites, *Geochim. Cosmochim. Acta*, *55*, 3831–3844.

Batchelor, J. D., S. J. K. Symes, P. H. Benoit, and D. W. G. Sears (1997), Constraints on the thermal and mixing history of lunar surface materials and comparisons with basaltic meteorites, *J. Geophys. Res.*, *102*, 19,321–19,334.

Bischoff, A., H. Palme, T. Geiger, and B. Spettel (1992), Mineralogy and chemistry of the EL-chondritic melt rock Ilafegh-009, *Lunar Planet. Sci.*, *XXIII*, 105–106.

Boggs, S., D. H. Krinsley, G. G. Goles, A. Seyedolali, and H. Dypvik (2001), Identification of shocked quartz by scanning cathodoluminescence imaging, *Meteorol. Planet. Sci.*, *36*, 783–791.

Burns, R. (1969), *Mineralogical Applications of Crystal Field Theory*, Cambridge Univ. Press, New York.

Cruikshank, D. P., D. J. Tholen, W. K. Hartmann, J. F. Bell, and R. H. Brown (1991), Three basaltic Earth approaching asteroids and the source of basaltic meteorites, *Icarus*, *89*, 1–13.

DeHart, J. M., and D. W. G. Sears (1988), Cathodoluminescence study of the Fayetteville and Plainview gas-rich regolith meteorites, *Meteoritics*, *23*, 265.

DeHart, J. M., G. E. Lofgren, Lu Jie, P. H. Benoit, and D. W. G. Sears (1992), Chemical and physical studies of chondrites: X: Cathodoluminescence and phase composition studies of metamorphism and nebular processes in chondrules of type 3 ordinary chondrites, *Geochim. Cosmochim. Acta*, *56*, 3791–3807.

Geake, J. E., G. Walker, D. J. Telfer, and A. A. Mills (1977), The cause and significance of luminescence in lunar plagioclase, *Philos. Trans. R. Soc. London, Ser. A*, *285*, 403–408.

Götze, J., M. R. Krbetscheck, D. Habermann, and D. Wolf (2000), High-resolution cathodoluminescence studies of feldspar minerals, in *Cathodoluminescence in Geosciences*, edited by M. Pagel et al., pp. 245–270, Springer-Verlag, New York.

Guimon, R. K., S. J. K. Symes, D. W. G. Sears, and P. H. Benoit (1995), Chemical and physical studies of type 3 chondrites XII: The metamorphic history of CV chondrites and their components, *Meteoritics*, *30*, 704–714.

Haq, M., F. A. Hasan, D. W. G. Sears, C. B. Moore, and C. F. Lewis (1989), Thermoluminescence and the origin of the dark matrix of Fayetteville and similar meteorites, *Geochim. Cosmochim. Acta*, *53*, 1435–1440.

Howard, E. C. (1802), Experiments and observations on certain stony substances, which at different times are said to have fallen on the Earth; also on various kinds of native iron, *Philos. Trans.*, *92*, 168–212.

Huang, Shaoxiong, Lu Jie, M. Prinz, W. K. Weisberg, P. H. Benoit, and D. W. G. Sears (1996), Chondrules: Their diversity and the role of open-system processes during their formation, *Icarus*, *122*, 316–346.

Krbetscheck, M. R., J. Götze, A. Dietrich, and T. Trautmann (1997), Spectral information from minerals relevant to luminescence dating, *Radiat. Meas.*, *27*, 6748–6965.

Lusby, D., E. R. D. Scott, and K. Kiel (1987), Ubiquitous high FeO-silicates in enstatite chondrites, *Proc. Lunar Planet. Sci. Conf. 17th*, Part 2, *J. Geophys. Res.*, *92*, E679–E695.

Machel, H. G. (2000), Application of cathodoluminescence to carbonate diagenesis, in *Cathodoluminescence in Geosciences*, edited by M. Pagel et al., pp. 271–302, Springer-Verlag, New York.

Marshall, D. J. (1988), *Cathodoluminescence of Geological Materials*, 146 pp., Chapman and Hall, New York.

Matsunami, S., et al. (1993), Thermoluminescence and compositional zoning in the mesostasis of a Semarkona group A1 chondrule and new insights into the chondrule-forming process, *Geochim. Cosmochim. Acta*, *57*, 2101–2110.

McCoy, T. J., et al. (1993), Roosevelt County 075: A petrologic, chemical and isotopic study of the most unequilibrated known H chondrite, *Meteoritics*, *28*, 681–691.

McCoy, T. J., K. Keil, D. D. Bogard, D. H. Garrison, I. Casanova, M. M. Lindstrom, A. J. Brearley, K. Kehm, R. H. Nichols, and C. M. Hohenberg (1995), Origin and history of impact-melt rocks of enstatite chondrite parentage, *Geochim. Cosmochim. Acta*, *59*, 161–175.

McSween, H. Y. (1977a), Carbonaceous chondrites of the Ornans type: A metamorphic sequence, *Geochim. Cosmochim. Acta*, *41*, 477–491.

McSween, H. Y. (1977b), Chemical and petrographic constraints on the origin of chondrules and inclusions in carbonaceous chondrites, *Geochim. Cosmochim. Acta*, *41*, 1843–1860.

Metzler, K., A. Bischoff, and D. Stöffler (1992), Accretionary dust mantles on CM chondrites: Evidence for solar nebular processes, *Geochim. Cosmochim. Acta*, *56*, 2873–2897.

Olsen, E. J., T. E. Bunch, E. Jarosewich, A. F. Noonan, and G. I. Huss (1977), Happy Canyon: A new type of enstatite achondrite, *Meteoritics*, *12*, 109–123.

Pagel, M., V. Barbin, P. Blanc, and D. Ohnenstetter (2000), *Cathodoluminescence in Geosciences*, Springer-Verlag, New York.

Ruzicka, A., G. A. Snyder, and L. A. Taylor (2000), Crystal-bearing lunar spherules: Impact-melting of the Moon's crust and implications for the origin of meteoritic chondrules, *Meteorit. Planet. Sci.*, *35*, 173–192.

Scott, E. R. D., D. J. Barber, C. M. Alexander, R. Hutchison, and J. A. Peck (1988), Primitive materials surviving in chondrites: Matrix, in *Meteorites and the Early Solar System*, edited by J. F. Kerridge and M. S. Matthews, pp. 718–745, Univ. of Ariz. Press, Tucson.

Sears, D. W. G., J. M. DeHart, F. A. Hasan, and G. E. Lofgren (1990), Induced thermoluminescence and cathodoluminescence studies of meteorites: Relevance to structure and active sites in feldspar, in *Spectroscopic Characterization of Minerals and Their Surfaces*, *ACS Symp. Ser.*, vol. 415, edited by L. M. Coyne, S. W. S. McKeever, and D. F. Blake, pp. 190–222, Am. Chem. Soc., Washington, D. C.

Sears, D. W. G., J. D. Batchelor, Lu Jie, and B. D. Keck (1991), Metamorphism of CO and CO-like chondrites and comparisons with type 3 ordinary chondrites, *Proc. NIPR Symp. Antarct. Meteorol.*, *4*, 319–343.

Sears, D. W. G., Lu Jie, P. H. Benoit, J. M. DeHart, and G. E. Lofgren (1992), A compositional classification scheme for meteoritic chondrules, *Nature*, *357*, 207–210.

Sears, D. W. G., P. H. Benoit, and Lu Jie (1993), Two chondrule groups each with distinctive rims in Murchison recognized by cathodoluminescence, *Meteoritics*, *28*, 669–675.

Sears, D. W. G., Shaoxiong Huang, and P. H. Benoit (1995), Chondrule formation, metamorphism, brecciation, an important new primary chondrule group, and the classification of chondrules, *Earth Planet. Sci. Lett.*, *131*, 27–39.

Sippel, R. F., and A. B. Spencer (1970), Luminescence petrography and properties of lunar crystalline rocks and breccias, in *Proceedings of the Apollo 11 Lunar Science Conference*, vol. 3, edited by A. A. Levinson, pp. 2413–2426, Pergamon, New York.

Skinner, B. J., and F. D. Luce (1971), Solid solutions of the type (Ca, Mg, Mn, Fe)S and their use as geothermometers for the enstatite chondrites, *Am. Miner.*, *56*, 1269–1295.

Smith, J. V., and R. C. Strenstrom (1965), Electron-excited luminescence as a petrologic tool, *J. Geol.*, *73*, 627–635.

Steele, I. M. (1986), Compositions and textures of relic forsterite in carbonaceous and unequilibrated ordinary chondrites, *Geochim. Cosmochim. Acta*, *50*, 1379–1395.

Steele, I. M. (1989), Compositions of isolated forsterites in Ornans (C3O), *Geochim. Cosmochim. Acta*, *53*, 2069–2079.

Steele, I. M. (1990), Mineralogy of meteorites revealed by cathodoluminescence, in *Spectroscopic Characterization of Minerals and Their Surfaces*, *ACS Symp. Ser.*, vol. 415, edited by L. M. Coyne, S. W. S. McKeever, and D. F. Blake, pp. 150–164, Am. Chem. Soc., Washington, D. C.

Stevens Kalceff, M. A., M. R. Phillips, A. R. Moon, and W. Kalceff (2000), Cathodoluminescence microcharacterization of silicon dioxide polymorphs, in *Cathodoluminescence in Geosciences*, edited by M. Pagel et al., pp. 193–224, Springer-Verlag, New York.

Symes, S. J. K., D. W. G. Sears, D. G. Akridge, Shaoxiong Huang, and P. H. Benoit (1998), The crystalline lunar spherules: Their formation and implications for the origin of meteoritic chondrules, *Meteorol. Planet. Sci.*, *33*, 13–30.

Takeda, H., H. Mori, J. S. Delaney, M. Prinz, G. E. Harlow, and T. Ishii (1983), Mineralogical comparison of Antarctic and non-Antarctic HED (Howardites-Eucrites-Diogenites) achondrites, Mem, *Natl. Inst. Polar Res. Spec. Issue Jpn.*, *30*, 181–205.

Telfer, D. J., and G. Walker (1978), Ligand field bands of Mn^{2+} and Fe^{3+} luminescence centers and their site occupancy in plagioclase feldspars, *Mod. Geol.*, *6*, 199–210.

Tomeoka, K., and P. R. Buseck (1985), Indicators of aqueous alteration in CM chondrites: Microtextures of a layered mineral containing Fe, S, O, and Ni, *Geochim. Cosmochim. Acta*, *49*, 2149–2163.

Weisberg, M. K., M. Prinz, and R. A. Fogel (1994), The evolution of enstatite and chondrules in unequilibrated enstatite chondrites: Evidence from iron-rich pyroxene, *Meteoritics*, *29*, 362–373.

Wood, J. A. (1962), Olivine and pyroxene compositions in type II carbonaceous chondrites, *Geochim. Cosmochim. Acta*, *31*, 2095–2108.

Zhang, Y., Shaoxiong Huang, D. Schneider, P. H. Benoit, J. M. DeHart, G. E. Lofgren, and D. W. G. Sears (1996), Pyroxene structures, cathodoluminescence and the thermal history of the enstatite chondrites, *Meteorol. Planet. Sci.*, *31*, 87–96.

D. G. Akridge, Process Dynamics, 700 Research Center Boulevard, Fayetteville, AR 72701, USA. (glen.akridge@processdyn.com)

J. M. C. Akridge, Arkansas-Oklahoma Center for Space and Planetary Sciences, University of Arkansas, Fayetteville, AR 72701, USA. (jmakrid@hotmail.com)

J. D. Batchelor, Department of Science, Community College of Southern Nevada, Cheyenne Campus, Las Vegas, NV 89030, USA. (david_batchelor@ccsn.edu)

P. H. Benoit, J. M. DeHart, A. Meier, M. Penrose, and D. W. G. Sears, Department of Chemistry and Biochemistry, University of Arkansas, Fayetteville, AR 72701, USA. (pbenoit@uark.edu; ameier@uark.edu; mpenrose@uark.edu; dsears@uark.edu)

J. Brewer, Department of Mathematics, Emory College, Atlanta, GA 30322, USA. (jwbrewer@learnlink.emory.edu)

Lu Jie, World Minerals Inc., 2500 Miguelito Road, Lompoc, CA 94436, USA. (lu.jie@worldminerals.com)

B. D. Keck, Procter and Gamble, Procter and Gamble Plaza, Cincinnati, OH 45202, USA.

D. M. Schneider, Chemistry Department, Southwest Missouri State University, Springfield, MO 65804, USA. (dms989t@smsu.edu)

S. J. K. Symes, Department of Chemistry, University of Tennessee, Chattanooga, TN 37403, USA. (steven-symes@utc.edu)

Zhang Yanhong, Indiana Geological Survey, Indiana University, Urbana-Champaign, IN 61820, USA.